

Image Blur Simulation for the Estimation of the Behavior of Real Objects by Monitoring Systems

Daniil A. Loktev, Alexey A. Loktev, Alexandra V. Salnikova, Alexander N. Faulgaber, Marina A. Slepneva

Abstract—The paper is devoted to the study of algorithmic and mathematical apparatus that can allow solving the problems of detection, capture and recognition of the objects of various classes. It can also help to determine the geometric, kinematic and dynamic parameters of the state and behavior of such objects within a wide range of possible values. In the study, the algorithmic support is developed allowing processing a series of primary images to generate patterns (mapping). The pattern mapping features are then used as informative parameters. Accounting for the fact that the graphic data formats are among the largest ones, one understands that, for the modern data processing systems, graphic data processing is a rather complex operation involving both the computationally intensive formalization of the obtained data in the form of visual patterns and the processing time minimization. The proposed image analysis can make it possible to reduce the cost of the procedure for obtaining the parameters of the moving objects in comparison with the methods currently in the wide use. Acceptable accuracy will still be ensured. Also, this method does not require a diversity of equipment to determine the largest number of object parameters and to present the obtained data in a uniform format. The paper considers how the blur pattern may appear in the object image and tests the possibility of its processing to obtain data on the geometric, kinematic and dynamic parameters of the real object behavior.

Index Terms—Measurement and monitoring system, image analysis, medium parameters, pattern boundary layer, motion blur, probability of error, simulation

I. INTRODUCTION

All the aspects of the current state of such branches of

Manuscript received May 24, 2021; revised January 26, 2022. This work was financially supported by the Ministry of Science and Higher Education of the Russian Federation (research project No. FSWF-2020-0022)

D. A. Loktev is an Associate Professor of the Department of Information Systems and Telecommunications, Bauman Moscow State Technical University, Moscow, Russia (corresponding author, phone: +7-499-263-62-86; fax: +7-499-263-66-25; e-mail: dn.al.loktev@mail.ru).

A. A. Loktev is a Professor and a Chairperson of the Department of Transportation Engineering, Russian University of Transport (MIIT), Moscow, Russia (e-mail: aaloktev@yandex.ru).

A. V. Salnikova is a PhD candidate of the Department of Electronics and Nanoelectronics, National Research University "MPEI", Moscow, Russia (e-mail: amicus.lat@yandex.ru).

A. N. Faulgaber is a Research Engineer of the Department of Electronics and Nanoelectronics, National Research University "MPEI", Moscow, Russia (e-mail: lytalalexandr@mail.ru).

M. A. Slepneva is a Leading Researcher of the Department of Electronics and Nanoelectronics and a Chairperson of the Department of Foreign Languages, National Research University "MPEI", Moscow, Russia (e-mail: slepnevama@mpei.ru)

human economic activity as transport, construction, industrial production and security can be characterized by the generation of the primary data on the studied objects, including the ones that are monitored and controlled in automatic mode. The tendency of automating the data array generation at the very earliest stages of operation of software and hardware complexes is displayed by a wide range of data-measuring and control systems. Such systems deal with obtaining, processing and application of data both on the operation of technical and technological processes and on the state and behavior of natural and man-made objects and phenomena [1].

A number of issues must be resolved before automated monitoring systems can be properly designed, built, and operated. Among these issues is determining the parameters of the state and behavior of the desired objects relative to the monitoring complex. They include the distance between the hardware installation and the desired object, the size and shape of the object, its speed and direction of its motion. The choice of the criteria providing a correct classification of the desired objects is another issue.

Obtaining primary data in such systems can be realized through the technical modules emitting electromagnetic waves in various frequency ranges and processing the radiation reflected from the studied object. Different types of equipment such as ultrasonic diagnostics systems, echolocation systems, laser range finders, various satellite and ground tracking systems are designed based on this very principle. Another way to extract primary data on the studied object is to process image patterns obtained by visual-optical, visual, television, photo and video supervisory control systems, night viewing systems, etc. The image generation can be carried out not only in the visible optical range, but also within the infrared (thermal imagers) and ultrasonic (underwater echolocation) spectrum. The control and monitoring complexes considered in the present paper are the nondestructive testing systems, since there are no direct impacts on the object that can cause its deformation and the changes in its performance characteristics. Such systems implement the second method for extracting primary data by generating a series of images of the studied object and the environment around it with their subsequent analysis [2]-[5].

At the same time, the data extracted during object image processing is the closest one to the patterns that the human brain forms and processes. No active devices emitting electromagnetic radiation of certain wavelengths that consume significant energy and affect the environment and living organisms are required. And thus one will also not

face the danger that such devices could be detected by the third-party systems that interfere into the operation of monitoring and control systems and sometimes explicitly oppose data and measurement processes.

II. THE MOST COMMON METHODS OF DATA ACQUISITION FROM THE OBJECT IMAGE

One of the most widely used visual methods is the stereoscopic vision application [6]. But in this case some difficulties may arise due to a high stereo system setting sensitivity and a number of additional procedures that appear necessary. The calibration of the cameras and the rectification of the images they produce are among them [7].

By the image of the object, one can estimate the distance to it, as well as its speed. It is accomplished through estimating the image blur: when the object is in the focus of the optical system, its image is the sharpest one, while the other object positioning leads to vivid blurring displaying itself in the circles of unsharpness.

To get data on an object by means of blur estimation, one can present the object visual image as the set of complex Haar's primitives and use wavelet analysis of the greatest possible number of images to fully evaluate the sharpness. Such approach has entirely proved its feasibility in the cases when it is the video- and photo fixation system that is in motion but not the observed object.

A refined estimation of the signal blur becomes possible when one carries out the double synthesized image blurring by applying the functions with the common Gaussian cores σ_a and σ_b that leads to generating the signals b_a and b_b whose reduced difference is then calculated [8]:

$$r(x) = [b(x) - b_a(x)] / [b_a(x) - b_b(x)].$$

There the function $r(x)$ will have its maximum values in the points where the blur simulation signal amplitude changes considerably. It allows calculating the blur σ , that can be considered as remaining the same within the total image area. If the condition $\sigma_a \sigma_b > \sigma$ holds, then the expression for the general blur takes the form:

$$s \gg s_a s_b / [(s_b - s_a) r_{\max}(x) + s_b].$$

After that, one can produce the depth map for the motionless object according to the chart suggested in Fig. 1.

While estimating the blurring of the motionless object (its speed is substantially lower than the speed of the camera) and when the moving photodetector is used, the expression $\sigma = f \Delta Y / r = f v \Delta t / r = f v / k r$ is applicable where f is the focus distance of the photodetector; ΔY is the actual motion distance of the object at the speed v and the time Δt ; r is the distance from the photodetector to the object; k is the number of the frames per second that the image pattern demonstrates.

The radius of the blur appearing due to the camera

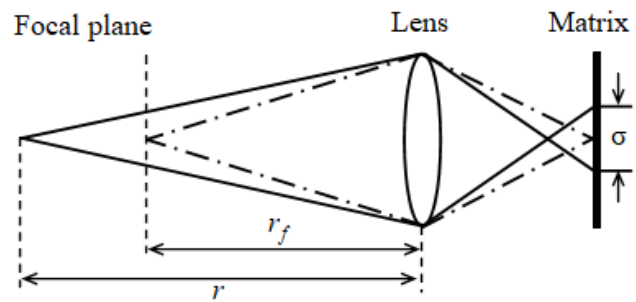


Fig. 1. Model of defocusing in the optical system.

motion is defined as $\sigma = f m / r$ where f is the focus distance; m is the distance of the photodetector shift during the exposure time t ; and d is the distance between the photodetector and the observed object.

To make the methods of object detection and identification universal even under the different conditions limiting their application field, their aggregation should be implemented. That will allow data acquisition depending on the environment and the characteristics of the observed object. Such approach results in a minimum number of possible errors thus improving the data quality.

III. FACTORS AFFECTING THE GENERATION OF THE BLURRED IMAGE PATTERNS

During operating automated monitoring systems receiving and processing object images, the tasks are solved of detecting the object pattern boundaries, improving the contrast, sharpness and clarity of these patterns, suppressing noises, etc. In the general case, the image processing procedure includes the following stages: extracting a separate image from a sequence of frames; detecting object patterns within a general image; correcting the parameters of the external environment; pattern capturing; determining the mapping parameters; recognizing the objects; identifying the parameters of the state and behavior of the desired object by analyzing a certain image or a series of images; and carrying out a statistical analysis of the results obtained [9], [10].

Machine vision systems and automated monitoring and control systems receiving and processing graphic data presented in photo and video formats deal with a number of image analysis issues concerning the representation of a 3D space fragment in the form of a 2D picture at a certain time moment [1], [4], [9].

When receiving the primary image, the quality of its graphic elements may be affected by various brightness and geometric parameters of the individual object patterns within a general image (the gradients of brightness, color, texture, shape, size, the presence of the shadow effects, etc.). Important are the changes in the general arrangement of objects in each separate image belonging to the particular series. Such factors as the changes in brightness and at the background, the presence or absence of the interferences between the observer and the desired object, the changes in the parameters of the state and behavior of the objects, the presence of atmospheric precipitation, the solid particles

suspended in the environment, various noise effects, etc. should be considered with great attention. The parameters of primary processing of the original image by a photo or video detector as well as the characteristics of the file write format must also be taken into account [11]-[13].

An important parameter characterizing both the general image and the object patterns located within it is the state of the boundary layer between various graphic patterns in the frame. In fact, the boundary layer is a blurred region that can be described as a function of some expansion of the object image primary element within the general image [13], [14]. The traditional approach to determining the blur degree states that when an object is in the focus of the optical system, its pattern is not blurred, but when the object is located closer to or further away from the indicated position, there has been blurring of the object pattern [14], [15]. The blur function in different directions can be determined using a circle of unsharpness. But the obtained image size together with the number and size of the photosensitive elements of the sensor must be accounted for. The algorithm for estimating the pattern blur by analyzing its boundaries exploits the image re-blurring using the Gaussian function with a priori known parameters. Further, the gradients of the original and synthesized images are compared and the estimate of the blurred object boundaries is calculated (Fig. 2) and then applied to the entire object pattern [16], [17].

To determine the blur degree of the desired object boundaries, it is sometimes proposed to represent the image as the dependence of the intensity upon the coordinates $I(x, y)$. Then, using the different levels of resolution of the Bokeh iterative procedure [18], [19], one should perform a number of operations: calculate, first, the first-order derivatives with respect to each of the coordinates (the projection of the gradient on the x - and y -axes) and then the second-order derivatives describing the changes in the projections of the gradient on the x - and y -axes. After that one nulls them to find the points with the highest values of the intensity change rate at the coordinates x_0 and y_0 (blur center), and, finally, one determines the function inflection points $A_1(x_1, y_1)$ and $A_2(x_2, y_2)$ that are located close to the already calculated values x_0 and y_0 . Thus, the values of x_1 and x_2 will estimate the blur boundaries $\sigma_x = x_2 - x_1$ of the object along the x -axis, while the values y_1 and y_2 will estimate the blur boundaries $\sigma_y = y_2 - y_1$ of the object along the y -axis.

The use of the Bokeh iterative procedure in the algorithm is

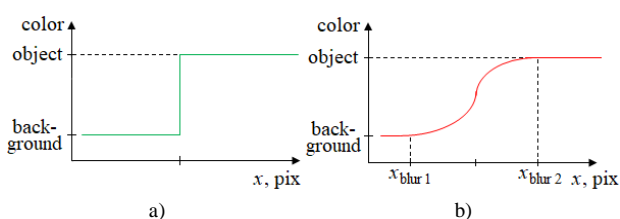


Fig. 2. The block diagram of the device for time sampling.

necessary for the analyzed points localization required to establish the boundaries both of the object and its blur. At each level of the iterative procedure, the derivatives of the first, second and third order of the image function $I(x, y)$ are determined, each of them calculated separately by x (assuming that $y = \text{const}$) and by y (assuming that $x = \text{const}$). Then, for each coordinate, a set of dependencies can be obtained, as it is shown in Fig. 3.

The function $I(x, y)$ describes the change in intensity by the x -coordinate. The first-order derivative estimates the intensity change rate by the x -coordinate (the projection of the gradient on the x -axis). The second-order derivative shows the change in the projection of the gradient on the x -axis. By nulling it, one can determine the point x_0 as the highest value of the intensity change rate by the x -coordinate (blur center). With the help of the third-order derivative, the points x_1 and x_2 are determined where the first derivative of the reference function changes sign (inflection points). That means that the rate of its change at these points neither decrease, nor increase when x -coordinate increases. Thus, the points x_1 and x_2 determine the boundaries of the object pattern blurring, that is, the blur region along the x -axis is $\sigma_x = x_2 - x_1$.

In fact, with any traditional representation of blur, this function limits the capabilities of detection systems, causes errors in the detection and recognition of an object, but it also provides additional data on the object that require correct processing [16], [20], [21].

Next, one should determine by how many iterations the algorithm using the Bouguet pyramid scheme will be faster than the one that does not use it. At the same time, the algorithm for estimating image blurring by finding derivatives of the first, second and third orders will remain the same.

In the case when an iterative Bouguet scheme is not applied and the analyzed original image is 2297 pixels wide and 4007 pixels high, the upper estimate of the computational complexity of the algorithm will be: $O(m, n) = \text{Width} \cdot \text{Height} = 2297 \cdot 4007 = 9204079$ cycles. But if the proposed iterative scheme is applied, the computational complexity will be:

$$O(m, n) = \text{Width} \cdot \text{Height} / 4^{L-3} = 3 + (2w_x^{L=2})(2w_y^{L=2}) \cdot 4 + (2w_x^{L=1})(2w_y^{L=1}) \cdot 4 + (2w_x^{L=0})(2w_y^{L=0}) \cdot 4 = 288 \cdot 501 + 16 \cdot 40 \cdot 40 + 16 \cdot 92 \cdot 92 + 16 \cdot 180 \cdot 180 = 823712$$

cycles. Here L is the resolution level, that is, in fact, the

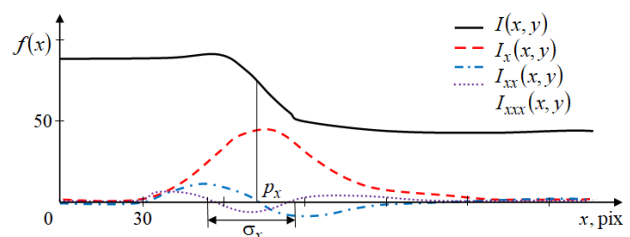


Fig. 3. Determining the object blur region along the x -axis.

algorithm iteration number; (w_x, w_y) is the neighborhood of the studied point, that is, the size of the frame around it, calculated along the axes x and y and depending on the algorithm iteration. As a result, the proposed iteration scheme can provide a performance boost of more than 11 times.

IV. MATHEMATICAL MODEL OF THE BLUR FUNCTION REPRESENTATION

In fact, blurring as a function is a certain expansion of the primary image element of the desired object. On the one hand, blur means a defective object pattern reception and/or a defective object pattern mapping. But, on the other hand, it constitutes an informative feature allowing obtaining data on the state and behavior of the desired object under various conditions of its localization and/or its pattern capture. Blur can determine the minimum range between the detected objects and the maximum speed of their motion which is crucial for their recognition. It can also help to define the parameters that are required for the photo and video detectors to operate in a remote control mode in monitoring or diagnostic systems under the specific conditions and when certain groups of controlled objects are involved [20], [22]. The factors that may influence blurring, i.e. blur degree will be presented further as specific patterns, and their main possible causes will be revealed.

It is proposed to describe a blur function using seven main factors. The first is the medium between the locations of the monitoring system and the desired object, and the blur caused by the medium is σ_{mat} . Then goes the color spectrum dependence which is actually the dependence upon the wave lengths of the corresponding range of the visible spectrum λ , thus here the blur caused by color spectrum is σ_{col} . The detection system elements in motion, i.e. the specific characteristics of motion of both the desired object and the monitoring system, constitute another factor. The blur caused by the motion of both the object and the monitoring system is σ_{mov} . The background state causes the blur σ_{bg} . The detector performance characteristics are responsible for the blur σ_{det} . The object image primary processing pattern produces the blur σ_{pp} . The state of the desired object surface cause the blur σ_{sc} .

General blur can be represented as a function that merges all the above types of blur:

$$\sigma_{\Sigma} = f(\sigma_{mat}, \sigma_{col}, \sigma_{mov}, \sigma_{bg}, \sigma_{det}, \sigma_{pp}, \sigma_{sc}).$$

The modern software applications for processing the primary images make it possible to successfully deal with the sum of the separate blur components:

$$\sigma_{\Sigma} = \sigma_{mat} + \sigma_{col} + \sigma_{mov} + \sigma_{bg} + \sigma_{det} + \sigma_{pp} + \sigma_{sc}.$$

If a different nature of one or another component of the blur function total is taken into account, then one can distinguish between the types of the blur. I.e., the blur

caused by the physical processes taking place in the medium where the object and the control system are located and the blur caused by the performance characteristics of the photodetector that captures the primary image. In this case, the final resulting blurring as a function can be represented in the form

$$\sigma_{\Sigma} = \sqrt{(\sigma_{mat} + \sigma_{col} + \sigma_{mov} + \sigma_{sc})^2 + (\sigma_{bg} + \sigma_{det} + \sigma_{pp})^2}.$$

The next step is to consider the influence of the medium between the locations of the studied object and the photodetector upon the blur function. It is fundamentally related to the varying transparency of various mediums for different wavelengths. The nonlinear dependence of the phase coefficient $\beta(\lambda)$ within the spectrum of available wavelengths (colors present in the image) should also be accounted for. The nonlinearity of the function $\beta(\lambda)$ depends upon the blur for each of the available colors, as well as upon the transparency function changes for different wavelengths at the range between the detector and the studied object [16], [23].

In general, blur caused by the parameters of the medium between the monitoring system and the desired object can be determined by the formula

$$\sigma_{mat} = (\Delta\lambda L \lambda / H v_f) d^2 P_{tr} / d\lambda^2. \quad (1)$$

In (1), the notations are the following: $\Delta\lambda$ is the range of wavelengths corresponding to the color components available in the image; P_{tr} is the transparency function of the medium depending upon the refractive index, the illumination and the presence of temperature fronts and various noises, for this case one can write the expression: $P_{tr} = P_{ref} + P_{ill} + P_{tf} + P_{ns}$; L is the reduced range to the object; H is the reduced characteristic size of the object; λ is the wavelength for a specific color; v_f is the group reduced velocity of the wavelength emission propagation in the available medium.

The medium transparency function can often be described by a dependence smoothly evolving from the central axis of the photodetector (which is the shortest range from the detector to the trajectory of the studied object) to the image boundary. This dependence is formed by the reduced distance from the detector to the object, the characteristic size of the object itself as well as the primary image size:

$$P_{tr}(L) = P_{tr}^0 \left[1 + K_{sp} \left(\frac{P_{tr}^0}{P_{tr}^m} \right) (L/H_m)^n \right].$$

Here n is the nonlinearity index showing the degree of change in the parameters of the medium between the edges of the primary image; P_{tr}^0 is the transparency function on the central axis of the photodetector; K_{sp} is the coefficient

that takes into account the change in the space metrics when this space is mapped in the form of a flat image; P_{tr}^m is the averaged transparency function for the reference shooting situation; H_m is the reduced width of the space at the level of the studied object that hits the primary image.

The dependence of blur upon color is, in fact, the dependence upon the wavelength of the corresponding range of the visible spectrum λ . Its nature is close to the nature of the previous component of the blur function and is related to the peculiarities of propagation of different wavelengths in space:

$$\sigma_{col} = \Delta\lambda L K_{col} P_{tr}^2 / H v_f \lambda,$$

where K_{col} is the vector of the functional coefficients that determine the features of various layers of the medium between the detector and the studied object in comparison with a certain reference layer.

The blur caused by the motion of the elements of the detection system is determined using the following scheme graphically displaying the appearance of the blurred points of the object pattern resulting from the motion of both the object and the photodetector. When choosing a system for detecting objects, the time for obtaining a photo-fixation frame should be commensurate with the time it takes for the object to move a distance between the two points in space. Here it is presupposed that the trajectory of this movement is close to a straight line [24], [25].

The generation of blur during the motion of the desired object and the detector of the monitoring system is demonstrated in Fig. 4. Here the object is highlighted by a circle, while the detector of the monitoring system – by a square. As the process of obtaining the primary image takes some time, the blur σ_{mov} is proposed to be considered as some function showing the relationship between the state

parameters of the detection system and the studied object obtained during the time between the beginning and the end of the initial image reception. During this time, both the object and the detector can move a certain distance. Thus, one considers the geometric relationship between the positions of the object and the detector during the reception of the image.

The motion is shown by arrows. One can also see there the distances between the objects and the perpendicular straight lines related to them. These lines are necessary to construct the blur projection onto the plane perpendicular to the camera axis – that is, the segment linking the position of the detector and the point of the object. These distances and lines are drawn by solid lines at the beginning of the detection and by dotted lines at the end of the image reception. The displacement of the object and the photodetector is proposed to be determined relative to the planes perpendicular to the segments linking the positions of the object and the detector at the beginning and the end of the process of obtaining the primary image. Such representation is chosen because the image itself and the blurring of separate patterns in it are mostly clear on the camera axis (in the plane perpendicular to the direction of detection). The displacement of the object and the photodetector of the monitoring system in a projection on the planes perpendicular to the segments linking the positions of the object and the photodetector at the beginning and the end of the image reception process can be represented as

$$\begin{aligned} l_{ob} \cos \varphi'_{ob} &= \sigma'_{ob}, & l_{ob} \cos \varphi''_{ob} &= \sigma''_{ob}, \\ l_{sy} \cos \varphi'_{sy} &= \sigma'_{sy}, & l_{sy} \cos \varphi''_{sy} &= \sigma''_{sy} \end{aligned} \quad (2)$$

or

$$\begin{aligned} l_{ob} &= \sigma'_{ob} / \cos \varphi'_{ob} = \sigma''_{ob} / \cos \varphi''_{ob}, \\ l_{sy} &= \sigma'_{sy} / \cos \varphi'_{sy} = \sigma''_{sy} / \cos \varphi''_{sy}. \end{aligned} \quad (3)$$

Here l_{ob} , l_{sy} are the ranges traveled by the studied object and the photodetector of the monitoring system during the time from the beginning to the end of receiving the primary photographic image; σ'_{ob} , σ''_{ob} and σ'_{sy} , σ''_{sy} are the blurs resulting from the displacement of the studied object (subscript *ob*) and the photodetector (subscript *sy*) in the projections on the planes perpendicular to the segments linking the positions of the object and the detector at the beginning (one superscript stroke) and the end (two superscript strokes) of the primary image reception time interval; φ'_{ob} , φ''_{ob} and φ'_{sy} , φ''_{sy} are the angles between the direction of displacement of the object (subscript *ob*) and the photodetector (subscript *sy*) and the planes perpendicular to the segment linking the initial position of the object and the detector (one superscript stroke), or to the segment linking the final position of the object and the detector (two superscript strokes) (Fig. 4).

The blur resulting from the motion of the object and the

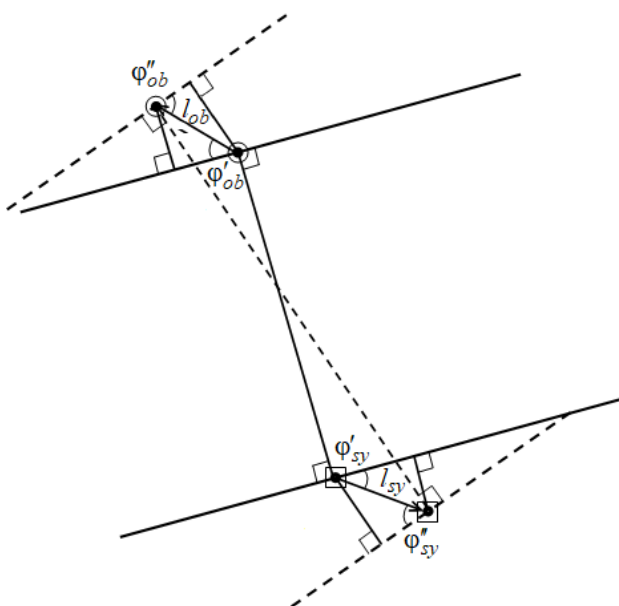


Fig. 4. The scheme of the generation of the blurred points of the object image resulting from the motion of the detector and the studied object.

photodetector, represented by the expressions (2) or (3) depends on the moments of beginning and ending of the primary image generation as well as on the type of the photodetector. Thus, it can be found as follows:

$$\sigma_{mov} = (\sigma'_{ob} + \sigma''_{ob}) + (\sigma'_{sy} + \sigma''_{sy})$$

or

$$\sigma_{mov} = \max_{\sigma'_{ob}, \sigma''_{ob}} (\sigma_{ob}) + \max_{\sigma'_{sy}, \sigma''_{sy}} (\sigma_{sy}).$$

One should specify the function describing the relationships between the final object blurred pattern and the motion of both the studied object and the photodetector of the control system taking into account their different locations at the time that determines the beginning and the ending of the primary image reception. This choice significantly depends on the parameters of the detector and can be determined empirically [26], [27]. When the size of the object pattern is larger than a certain threshold value, one should consider the aberrations (blur) that occurs due to the linear size of the object.

The generation of the blurred image fragments is also possible due to their remoteness from the axis of the photodetector and it is related to the angle θ_1 between the axis of the photodetector and the line linking the detector (as a point) and the end point of the studied object:

$$L^2 + H^2/4 = L^2/\cos^2 \theta_1.$$

If the blur on the axis of the photodetector is conditionally taken as a minimum, then, in the case of the medium parameters linearly changing along the full width of the object, the following ratio is valid:

$$\sigma_{sz} = \sigma_{ex} - \sigma_{ax} = LP_{tr}^{ex}/v_f \cos \theta_1 - LP_{tr}/v_f.$$

Here P_{tr}^{ex} is the transparency function of the medium at the level of the outermost point of the studied object.

If the size of the object pattern is greater than a certain threshold value corresponding to the distance from the detector L_d , then the following relations can be written

$$\sigma_{sz} = \begin{cases} LP_{tr}^{ex}/v_f \cos \theta_1 - LP_{tr}/v_f, & \text{if } L < L_d, \\ \sqrt{LL_d} P_{tr}^{ex}/v_f \cos \theta_1 - LP_{tr}/v_f, & \text{if } L \geq L_d. \end{cases} \quad (4)$$

The distance L_d is determined empirically for each specific case of obtaining a series of primary images.

In the case of the medium parameters changing along the width of the studied object, instead of the expressions (4), the following relations are used:

$$\sigma_{sz} = \begin{cases} L(P_{tr}^{ex})^g/v_f \cos \theta_1 - L(P_{tr})^g/v_f, & \text{if } L < L_d, \\ \sqrt{LL_d}(P_{tr}^{ex})^g/v_f \cos \theta_1 - L(P_{tr})^g/v_f, & \text{if } L \geq L_d. \end{cases}$$

Here the exponent g is the parameter that determines the gradient of the change in the medium properties in the direction perpendicular to the detector axis. It should be noted that if it is necessary to calculate the blur σ_{sz} , then it is added to the blur σ_{mov} and further they are both taken into account in the forthcoming calculations.

The very concept, the definition of the “background” makes an important factor in determining the influence of the background on the object pattern blurring (σ_{dg}). In this paper, everything located around the boundaries of the desired object is considered a background, without taking into account the depth of the spacing of the separate background elements [23], [28]. A special case is the case of an “ideal” background in the form of a monochrome, black-and-white or more complex image located at a certain distance behind the studied object. Different background designs and textures depending upon the parameters of the state and behavior of the desired object can also be used, otherwise the “ideal” background can be obtained and its application can be substantiated based on the principles of geometrical optics, Huygens-Fresnel and Fraunhofer as well as on the estimates of the possible aberrations and deviations.

The calculation of the blur resulting from the certain parameters and characteristics of the detection equipment (σ_{det}) and the primary processing of the object pattern (σ_{pp}) is carried out by means of in situ experiments using the specified photodetectors and cameras and the presentation formats that they support [29], [30]. The influence of the state and behavior of the studied object surface on blurring (σ_{sc}) is not considered, since the solid-state objects are detected and their shape and color do not change during observation. The situations of dynamic contact between the objects leading to their subsequent deformation are also not examined.

The presented mathematical model for the blurring of the object pattern elements takes into account many different parameters. This leads to difficulties in determining the influence of each factor. For the convenience of conducting a comparative analysis for some classes of applied problems, it is proposed to use the blur function $\sigma_{\Delta\lambda L}$ reduced to a unit of distance and a unit of a color range:

$$\sigma_{\Delta\lambda L} = K_{sp} (\lambda^2 d^2 \beta / d\lambda^2 + 2\lambda d\beta / d\lambda) / v_f,$$

where K_{sp} is the coefficient that determines the geometric parameters of the space near the object; β is the characteristic of the color mapping in space.

The characteristic of the color mapping in space can be represented as $\beta^2 = (N^2/P_{tr}^{pr} - M^2)/H_m^2$, where

$N = kH_m \sqrt{P_{tr}/P_{tr}^{ax}}$, P_{tr}^{ax} is the function of the medium transparency on the detector axis towards the studied object; $k = 2\pi/\lambda$, k is the wave number in a free space; M is the parameter of a separate color component transfer in space which can be determined using the Gaussian approximation in the following way:

$$M^2 = \frac{k_1}{H_0^2} \int_0^\infty \left[\left(\frac{dF_0(H)}{dH} \right)^2 + N^2 f(H) F_0^2(H) \right] H dH.$$

Here $f(H)$ is the dependence that determines the gradient of the function of transparency in the direction perpendicular to the segment “detector-studied object”, while H_0 is the reduced transverse dimension of the object pattern. It should be noted that the polynomial form of the dependence $f(H)$ is most widely used as it is determined based on the real conditions for obtaining the primary image, but the procedure of $f(H)$ linearizing can also be implemented for the small space linear dimensions.

V. THE APPLICATION OF THE PROPOSED SOFTWARE FOR THE OPERATION OF THE VEHICLE MONITORING SYSTEM

For the specific conditions of using the data-measuring control and monitoring system with the specified classes of the desired objects, the correlations between the separate components of the blur function can change significantly, taking into account certain intervals of measured values of the parameters of the state and behavior of the objects. It allows simplifying the model for determining the blurred object pattern, and, more than that, separate components even may be neglected due to their low values relative to the other terms.

In Figs. 5, 6, there are shown the primary images of a vehicle which is the object for monitoring moving in a braking mode so that its speed decreases from about 45 km/h to 20 km/h. Thus, in the process of receiving primary patterns with the same photodetector settings, the blur function is generated, with its components σ_{mov} and σ_{det} being prevalent. For the images presented in Fig. 5, the photodetector is fixed and focused on the lane along which the car is moving. The images presented in Fig. 6a and 6b are obtained when the defocused photodetector is moving in the direction opposite to the vehicle motion at the speed of about 45 km/h.

In Fig. 5, the object image corresponds to the focusing of the photodetector on the driving lane along which the car is moving so that the value of the blur function is the lowest one and is determined by the component σ_{det} . From the joint review of the blurred object patterns presented in Fig. 5, 6, it can be seen that the influence of the blur function components σ_{det} , σ_{col} and σ_{bg} is really significant. Thus, Fig. 6a shows an example of blurring due to a camera movement. In Fig. 6b, one can see a blurring due to camera defocusing. Subsequent analysis of the object image



a)



b)

Fig. 5. The primary images of the moving object with the fixed photodetector focused on the specified driving lane: a) at the beginning of the detector's field of view; b) at the end of the detector's field of view.



a)



b)

Fig. 6. The primary images of the moving object: a) when the photodetector is moving in the opposite direction; b) when the photodetector is fixed and focused on the point that is 2 meters away from the operator.

blurring in the case when the internal characteristics of the camera are known allows determining the distance to the object, its dimensions, and its speed and movement direction. Thus, this paper considers the possibility of extracting useful data from the noise component of the original signal, such as image blurring.

VI. DETERMINING THE CHARACTERISTICS OF THE MOVING OBJECTS

It is useful to approximate the experimentally obtained numerical data on the dependences defining the degree of blurring of the object boundaries by a sixth-degree Lagrange polynomial [31]. The polynomial coefficients are determined using a convolutional neural network [32], [33].

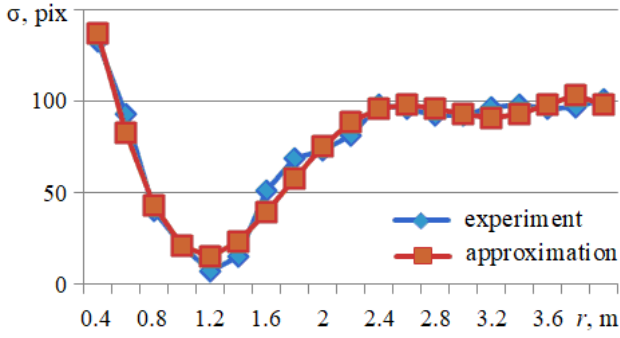


Fig. 7. The approximation of the experimental data by polynomial dependence with a focus point of 1.2 m.

Thus, the following expression can be obtained for the focus point of 1.2 m (the coefficient of determination is $R^2 = 0.96$) while the focus length is equal to 52 mm (Fig. 7):

$$\begin{aligned} \sigma_i = & -5.95r_i^6 + 76.21r_i^5 - 360.87r_i^4 + \\ & + 743.59r_i^3 - 525.14r_i^2 - 148.94r_i + 241.8. \end{aligned} \quad (5)$$

In (5), the notations are the following: σ_i is the blur of the i -th point of the object boundaries and r_i is the distance of the i -th point of the object from the camera.

The distance to the real object can be defined as the distance to the point with the minimum coordinate r_{\min} of the set of distances P_r to the points of the object surface [28], [34].

After determining the set of the distances P_r to the surface points of the object Ob , one can estimate its size. The object size is presented as the difference between the maximum and the minimum coordinates in each of the 3 dimensions. For this purpose, after determining the contour C of the object Ob , one defines its length l (the horizontal dimension), height h (vertical dimension) and width w (it is estimated by the distance from the camera) during the consistent contour bypass:

$$\begin{aligned} l = & \max_{P \in C} \{P_x\} - \min_{P \in C} \{P_x\}, & h = & \max_{P \in C} \{P_y\} - \min_{P \in C} \{P_y\}, \\ w = & \max_{P \in C} \{P_r\} - \min_{P \in C} \{P_r\}, \end{aligned}$$

where P is the set of the contour points and P_x , P_y and P_r are the sets of the corresponding coordinates x , y , z of the points of the contour C .

To determine the speed, a set of three components v_x , v_y , v_z is considered. The axes x and y pass in the image plane while the axis z is directed perpendicular, “into” the image. Then

$$\Delta\beta_{ob}/\beta_{frame} = \Delta X_{ob}/W_{frame}.$$

From the right-angled triangle shown in Fig. 8, it follows that

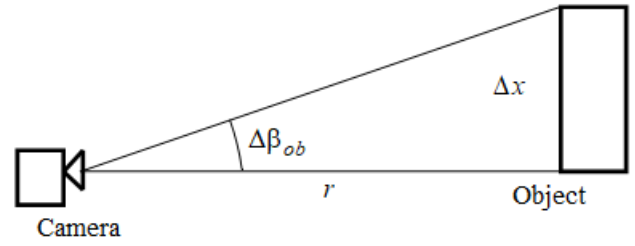


Fig. 8. Calculating the change in the viewing angle of an object from a right-angled triangle.

$$\tan \Delta\beta_{ob} = \Delta x/r.$$

At small angles $\Delta\beta_{ob}$ one gets

$$\Delta x = r\Delta\beta_{ob} = \beta_{frame}\Delta X_{ob}r/W_{frame}.$$

Their estimates can be obtained by dividing the biases in the video stream by the time interval $N\tau$:

$$\begin{aligned} v_x = & \beta_{frame}\Delta X_{ob}l/W_{frame}N\tau, \\ v_y = & \alpha_{frame}\Delta Y_{ob}l/H_{frame}N\tau, \\ v_z = & [l(\sigma, t) - l(\sigma, t - N\tau)]/N\tau. \end{aligned}$$

Here ΔX_{ob} , ΔY_{ob} describe the shift of the object center relative to the background that is expressed in pixels for N frames; W_{frame} and H_{frame} are the width and the height of the frame; β_{frame} and α_{frame} are the horizontal and vertical viewing angles of the camera; τ is the frame duration; l is the distance to the object determined from expressions (5). Then the overall speed is calculated by the formula:

$$v = \sqrt{v_x^2 + v_y^2 + v_z^2}.$$

During the experimental studies carried out using a moving vehicle (car), the vehicles are considered with a greater and lesser difference between the average intensity of the whole picture and the average intensity of the moving object pattern that can be calculated by the three color components [29], [35]. One presents both the comparison of the results of application of the proposed methods modified based on the characteristic points and the building of cascade classifiers. One also finds the probabilities of the type I (P_1) and type II (P_2) errors [36] depending on the speed V of the object observed using different contrasts (Figs. 9a, 9b).

The algorithm applying cascade classifiers is based on the AdaBoost algorithm, which consists in using Haar primitives and a set of reference objects [23]. Based on their synthesis, one more advanced and powerful classifier can be compiled. In the process of compiling or training the final classifier, the emphasis is on the standards that are recognized “worse”.

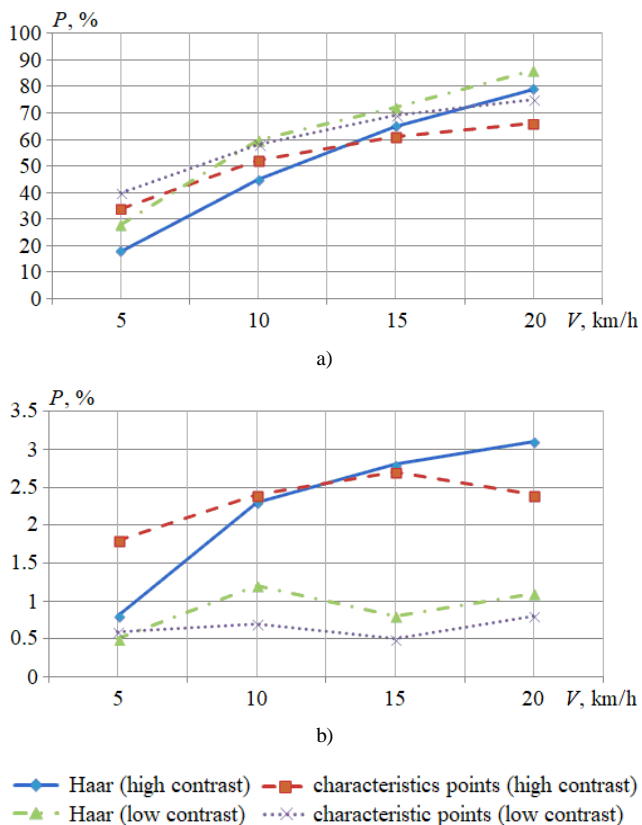


Fig. 9. The dependences of the probabilities of the type I (a) and type II (b) errors upon the speed of the objects with different contrasts.

AdaBoost calls a weak classifier in a loop and, after each call, the distribution of weights D_t corresponding to the importance of each of the objects of the training set is updated. At each iteration, the weights of any incorrectly classified object increase, the new classifier “focuses its attention” on these objects and minimizes the weighted classification error:

$$h_t = \arg \min_{h_j \in H} \varepsilon_t,$$

where $\varepsilon_t = \sum_{i=1}^m D_t(i) [y_i \neq h_j(x_i)]$ is a weighted classifier error h_t , if

$$\varepsilon_t \geq 0.5 \quad (6)$$

after which the algorithm execution stops (at another values of ε_t , the iteration goes on building the cascade classifier); x_i stands for the objects requiring an optimal classifier; h_j is the cascade classifier of the current iteration which can be considered as an optimal one, if the specified condition (6) holds.

Hereafter the resulting classifier is built:

$$H(x) = \text{sign} \left[\sum_{t=1}^T \alpha_t h_t(x) \right],$$

where $\alpha_t = \ln \left[\frac{1 - \varepsilon_t}{\varepsilon_t} \right] / 2$.

After choosing the optimal classifier h_t for the distribution D_t , objects x_i that are correctly identified by the classifier have weights smaller than the objects that are incorrectly identified. Therefore, when testing the classifiers for the distribution D_{t+1} , the algorithm will choose a classifier that better identifies objects incorrectly recognized by the previous classifier.

The method of recognizing objects by certain characteristic points uses the Harris-Laplace detector to determine these characteristic points and the Lucas-Canada method to calculate the optical flux in the neighborhood of the previously defined points for their subsequent tracking [19].

The object contrast k relative to the background is determined as $k = \text{abs}(I_{ob} - I_b) \lambda^d$, where I_{ob} and I_b are the average intensities of the object and the background, respectively, and λ is the coefficient that determines the external conditions (illumination, atmosphere transparency, etc.). The allowable minimum distance at which an object can be detected is $d = s \text{tg } \alpha$, where s is the maximum pixel size and α is the angular resolution of the camera used for observation.

It follows from Figs. 9a and 9b that the pattern recognition methods are fully operable and effective in the case of a high contrast object image. For example, Haar primitives and the motion tracking of the characteristic points [37] can be used in this case. When the image contrast with regard to the visible optical range is low, the object may be hard to recognize. Therefore, in such cases it is better to use the other methods of obtaining data on the object, for example, to carry out image processing in the infrared mode or with the help of the ultrasonic signals.

VII. CONCLUSION

Based on the introduced model for blurring both the whole object pattern and its separate elements, the mathematical and algorithmic support is developed that allows improving the parameters of the primary images, such as sharpness, contrast, lighting compensation, etc. This, in turn, makes it possible to increase the probability of detection and recognition of the objects under control in automated video monitoring systems.

The proposed model of the object pattern blurring enables the researchers to develop new approaches to the study of the blurred region boundaries between different objects and between an object and a background. The characteristics of these blurred region boundaries can determine not only the noise components of the image and be a quality criterion in determining the sharpness, contrast and clarity of a photograph. They can also carry important data on the state and behavior of the object itself. More than that, they can provide a general estimate of the operation of an automated monitoring and control system. The introduced techniques make it possible to calculate such a situation when some types of blur can be compensated for by others. They can also help to simulate and test the case

when the operator of the control and monitoring system manages to adjust the characteristics of the blur using hardware or/and software tools. Thus the possible ranges of detectable values can be increased and the accuracy of their determination can be improved.

REFERENCES

- [1] H. Wang, X. Zhang, L. Damiani, P. Giribone, R. Revetria, and G. Ronchetti, "Video analysis for improving transportation safety: obstacles and collision detection applied to railways and roads," in *Lecture Notes in Engineering and Computer Science: Proceedings of The International MultiConference of Engineers and Computer Scientists 2017*, 15-17 March 2017, Hong Kong, China, pp. 909-915.
- [2] G.G. Robertson, S.K. Card, and J.D. Mackinlay, "Information visualization using 3D interactive animation," *Communications of the ACM*, vol. 36, no. 4, pp57-71, 1993.
- [3] X. Tan and B. Triggs, "Local texture feature sets for face recognition under difficult lighting conditions," *IEEE Transactions on Image Processing*, vol. 19, no. 6, pp1635-1650, 2010.
- [4] Z. Sun, G. Bebis, and R. Miller, "On-road vehicle detection using optical sensors: A review," in *Proc. 7th International IEEE Conference on Intelligent Transportation Systems*, Washington, 2004, pp585-590.
- [5] N.J. Sugang, M. Ramos Jr., and N.A. Arriola, "Road surface obstacle detection using vision and LIDAR for autonomous vehicle," *Lecture Notes in Engineering and Computer Science: Proceedings of The International MultiConference of Engineers and Computer Scientists 2017*, 15-17 March 2017, Hong Kong, China, pp. 260-264.
- [6] C. Beder, B. Bartczak, R. Koch "A comparison of PMD-cameras and stereo-vision for the task of surface reconstruction using patchlets," in *Proc. 2007 IEEE Conference on Computer Vision and Pattern Recognition*, Minneapolis, 2007, pp1-8.
- [7] L. Nalpanitidis, G. Sirakoulis, and A. Gasteratos, "Review of stereo vision algorithms: From software to hardware," *International Journal of Optomechatronics*, vol. 2, no. 4, pp435-462, 2008.
- [8] H. Hu and G. Haan, "Low cost robust blur estimator," in *Proc. 2006 IEEE International Conference on Image Processing*, Atlanta, 2006, pp617-620.
- [9] M. Wiedemann, M. Sauer, F. Driewer, and K. Schilling, "Analysis and characterization of the PMD camera for application in mobile robotics," *IFAC Proceedings Volumes (IFAC-PapersOnline)*, vol. 18, no. 1, pp46-51, 2008.
- [10] M. Lindner and A. Kolb, "Calibration of the intensity-related distance error of the PMD TOF-camera", *Proceedings of SPIE – The International Society for Optical Engineering*, vol. 6764, pp56-64, 2007.
- [11] L. Lelegard, B. Vallet, and M. Bredif, "Multiscale haar transform for blur estimation from a set of images," *ISPRS Archives of the Photogrammetry, Remote Sensing and Spatial Information Sciences*, vol. 38, no. 3W22, pp65-70, 2013.
- [12] G. Chandan, A. Jain, H. Jain, and M. Mohana, "Real time object detection and tracking using deep learning and OpenCV," in *Proc. International Conference on Inventive Research in Computing Applications*, Coimbatore, 2018, pp1305-1308.
- [13] P.P. Koltsov, "Image blur estimation" (in Russian), *Computer Optics*, vol. 35, no. 1, pp95-102, 2011.
- [14] O.B. Braslavskaya, I.Yu. Gendrina, and A.S. Kvatch, "The comparison of two methods for determining of point spread function and optical transfer function" (in Russian), *Izvestiya Vysshikh Uchebnykh Zavedenii. Fizika*, vol. 56, no. 9-2, pp215-216, 2013.
- [15] P. Langley, "User modeling in adaptive interfaces," *Lecture Notes in Computer Science (including subseries Lecture Notes in Artificial Intelligence and Lecture Notes in Bioinformatics)*, vol. 407, pp357-370, 1999.
- [16] R. Huang, M. Fan, Y. Xing, and Y. Zou. "Image blur classification and unintentional blur removal," *IEEE Access*, vol. 7, pp106327-106335, 2019.
- [17] A.R. Puerta, "Issues in automatic generation of user interfaces in model-based systems," in *Proc. Second International Workshop on Computer-Aided Design of User Interfaces*, Namur, 1996, pp323-325.
- [18] D. Cremers and S. Soatto, "Motion competition: A variational approach to piecewise parametric motion segmentation," *International Journal of Computer Vision*, vol. 62, no. 3, pp249-265, 2005.
- [19] A. Bruhn, J. Weickert, and C. Schnörr, "Lucas/Kanade meets Horn/Schunck: Combining local and global optic flow methods," *International Journal of Computer Vision*, vol. 61, no. 3, pp211-231, 2005.
- [20] A. Loktev, V. Sychev, B. Gluzberg, and E. Gridasova, "Modeling the dynamic behavior of railway track taking into account the occurrence of defects in the system wheel-rail," *MATEC Web of Conferences*, vol. 117, pp1-6, 2017.
- [21] D.A. Loktev, A.A. Loktev, A.V. Salnikova, and A.A. Shaforostova, "Determination of the dynamic vehicle model parameters by means of computer vision," *Communications – Scientific Letters of the University of Zilina*, vol. 21, no. 3, pp28-34, 2019.
- [22] D.A. Loktev and A.A. Loktev, "Determination of object location by analyzing the image blur," *Contemporary Engineering Sciences*, vol. 8, no. 9, pp467-475, 2015.
- [23] D.A. Loktev and A.A. Loktev, "Development of a user interface for an integrated system of video monitoring based on ontologies," *Contemporary Engineering Sciences*, vol. 8, no. 20, pp789-797, 2015.
- [24] D.A. Loktev and A.A. Loktev, "Estimation of measurement of distance to the object by analyzing the blur of its image series," in *Proc. 2016 International Siberian Conference on Control and Communications*, Moscow, Russia, 2016, pp1-6.
- [25] D. Loktev, A. Loktev, R. Stepanov, V. Pevzner, and K. Alenov, "An aggregated method for determining railway defects and obstacle parameters," *IOP Conference Series: Materials Science and Engineering*, vol. 317, no. 1, pp012-021, 2018.
- [26] A.A. Loktev, V.G. Dmitriev, P.V. Sychev, V.A. Komkov, and B.V. Boytsov, "Analysis of methods for restoring the density distribution of random variables of assessing the condition of the railroad track according to the indicated values of the track recording car," *Asia Life Sciences*, vol. 9, no. 1, pp111-124, 2019.
- [27] D.A. Loktev and A.A. Loktev, "Diagnostics of external defects of railway infrastructure by analysis of its images," in *Proc. 2018 Global Smart Industry Conference*, Chelyabinsk, 2018, pp1-7.
- [28] A.A. Loktev, D.A. Loktev, and A.V. Salnikova, "The system of facial recognition in the infrared range," *Communications – Scientific Letters of the University of Zilina*, vol. 22, no. 1, pp95-101, 2020.
- [29] D.A. Loktev, Y.A. Bykov, and N.I. Kovalenko, "Use of the analysis technique of image blurring for detection of external defects of a railway track" (in Russian), *Science and Technology of Transport*, no. 1, pp69-75, 2016.
- [30] D. Loktev, A. Loktev, V. Korolev, I. Shishkina. "Mathematical modeling of blur of object in image for using it as information criterion", *Lecture Notes in Networks and Systems*, vol. 246, pp268-275, 2022.
- [31] O.V. Chernoyarov, M. Breznan, and A.V. Terekhov, "Restoration of deterministic and interference distorted signals and images with use of the generalized spectra based on orthogonal polynomials and functions," *Communications – Scientific Letters of the University of Zilina*, vol. 15, no. 2A, pp71-77, 2013.
- [32] S. Wang, D. Liu, Z. Yang, C. Feng, and R. Yao, "A convolutional neural network image classification based on extreme learning machine," *IAENG International Journal of Computer Science*, vol. 48, no. 3, pp799-803, 2021.
- [33] A. Alzu'bi, A. Amira, and N. Ramzan, "Learning transfer using deep convolutional features for remote sensing image retrieval," *IAENG International Journal of Computer Science*, vol. 46, no.4, pp637-644, 2019.
- [34] A. Loktev, V. Korolev, I. Shishkina, L. Chernova, P. Geluh, A. Savin, and D. Loktev, "Modeling of railway track sections on approaches to constructive works and selection of track parameters for its normal functioning," *Advances in Intelligent Systems and Computing*, vol. 982, pp325-336, 2020.
- [35] D.A. Loktev and A.A. Loktev, "Automated system for monitoring the upper structure of the railway track for extreme arctic conditions," *Lecture Notes in Civil Engineering*, vol. 49, pp205-214, 2020.
- [36] O.V. Chernoyarov, B. Dobrucky, A.V. Salnikova, and A.A. Makarov, "Detection and measurement of the unknown moment and magnitude of the Gaussian random process energy parameters abrupt change," *International Review on Modelling and Simulations*, vol. 12, no. 5, pp264-280, 2019.
- [37] P.A.S. Mendes, M. Mendes, A.P. Coimbra, and M.M. Crisostomo, "Movement detection and moving object distinction based on optical flow," *Lecture Notes in Engineering and Computer Science: Proceedings of The World Congress on Engineering 2019*, 3-5 July 2019, London, United Kingdom, pp. 48-53.